

Soumendu Bisoi, Arun Kumar Mandal, Asheesh Singh and Susanta Banerjee*

Gas separation properties of Troeger's base-bridged polyamides

DOI 10.1515/epoly-2016-0291

Received November 3, 2016; accepted December 7, 2016; previously published online January 20, 2017

Abstract: A series of new polyamides (PAs) has been prepared from a Troeger base-bridged diamine (TB), 2,8-diamino-4,10-dimethyl-6H,12H-5,11-methanodibenzo[1,5]-diazocine and different commercially available diacid monomers via the conventional polycondensation method. Dense membranes were prepared from the PAs by solution casting and solvent evaporation techniques. The synthesized PAs showed high glass transition temperature (283–290°C), 10% weight loss up to temperature 431°C in air, and tensile strength up to 91 MPa. The PA membranes showed higher permeability than some commercially used glassy polymers (P_{CO_2} up to 109 and P_{O_2} up to 21 Barrer) and permselectivity ($P_{\text{CO}_2}/P_{\text{CH}_4}$ up to 53.7 and $P_{\text{O}_2}/P_{\text{N}_2}$ up to 7.52) in comparison to many other PAs published in the literature.

Keywords: dielectric constant; gas transport properties; polymer membranes; solubilityselectivity; Troeger's base-bridged polyamides.

1 Introduction

In recent decades membrane technology has been sparked into a substantial research area in material design and development due to its technical advantages such as simple operation, energy savings, the flexibility of raw materials in membrane fabrication and scale up and tailoring (1–3). The potential application of this technology includes removal of CO_2 from non-polar gases (CH_4 and N_2), natural gas upgrading, natural gas sweetening (CO_2/CH_4) and N_2 or O_2 enrichment of air, are the key issues of environmental friendly and sustainable development for the next several decades (1, 3, 4). The key parameters for membrane separation performances are permeability

coefficients (P), the selectivity (α) and stable long-term separation properties. Thus, new membrane materials are required for higher gas throughput by improved permeability and selectivity (5). A polymer with a high fractional free volume (FFV) reduces the membrane area and the energy for a given volume of gas cause significant inter-chain separation thus, increase permeability and greater size selectivity could be obtained by increasing polymer chain rigidity and penetrant solubility selectivity value (6). But, polymeric membranes suffer from an obvious trade-off between the desired permeability and selectivity, as quantified by Robeson upper-bound relationship in 2008 (7). Nowadays, CO_2 has been considered as the largest and fastest growing contributor to climate change. As a result, industrial and academic research has been focused to design new polymers with improved CO_2 separation performances from power plants flue gases (3, 8). The number of CO_2 removal plants using commercial membranes is still rather limited, through research in the field is very active, and a large number of polymers have been developed (8, 9).

Aromatic polyamides (PAs) has been known as a super engineering plastic due to their excellent thermal, mechanical, corrosion resistance properties and are widely used in membrane-based gas separation industries. The main difficulty for traditional PAs and commercial material like Matrimid® and cellulose acetate are their low gas permeable with low-free-volume, although they possess high selectivity for most of the gas pairs (10–14). Recently, polymers of intrinsic microporosity (PIMs) were discovered which consist of rigid and contorted macromolecular structure which ensures high free volume and are rapidly expanding a class of solution-processable amorphous polymer (15–17). Different types of PIMs polymers with a bulky and kinked structure like spirobisindane (18), triptycene (19), Tröger's base (20, 21) have been reported. To develop PIMs for use in gas separation membranes, Tröger's base (TB) and its structural analogous are of regular interest as molecular building blocks for polymer preparation. TB-based PIMs exhibited the state-of-the-art performance in gas separation applications. TB is a bridge bicyclic diamine 2,8-dimethyl-6H,12H-5,11-methanodibenzo[b,f][1,5]diazocine (21). It is well-known that N-containing functional groups present in polymers could enhance the affinity of CO_2 . As a result

*Corresponding author: Susanta Banerjee, Materials Science Centre, Indian Institute of Technology, Kharagpur-721302, India, Tel.: +91-3222283972, Fax: +91-3222255303, e-mail: susanta@matssc.iitkgp.ernet.in

Soumendu Bisoi, Arun Kumar Mandal and Asheesh Singh: Materials Science Centre, Indian Institute of Technology, Kharagpur-721302, India

solubility of CO₂ in the polymer membrane increases which ultimately give rise to high solubility and selectivity. TB is fairly basic in nature, the in-built alkaline nitrogen atoms of tertiary amines in the TB unit contribute to the affinity between CO₂ molecules and the polymer membrane (22).

McKeown et al. synthesized rigid-bridged and non-planar bicyclic ladder-type TB polymer (e.g. PIM-EA-TB, PIM-Trip-TB and PIM-B Trip-TB, etc.). Those TB-based membranes had excellent gas permeability and remarkably high gas selectivities for O₂/N₂ gas pairs (23). Jin et al. constructed TB-derived microporous polyimides and copolymers, which show high-performances gas separation (20, 24). Lee et al. prepared TB-based PIM-PIs and reported gas transport properties (16, 25, 26). Recently, McKeown et al. reported a series of PIM-TB-PI derived from the methyl group containing TB diamine monomer (4MTBDA) for gas permeation measurements (27). The inclusion of rigidity and kink structure of the TB unit into the polymer backbone imparted intrinsic microporosity and improved the overall gas transport performance.

Although, a few TB-based polyimides of intrinsic microporosity (PIM-PIs) have been reported in the literature, TB-based PAs for membrane-based gas separation have not yet been reported. TB-derived polymers are designed to enhance the rigidity of the whole backbone and thus achieve improved performance. TB units with intrinsic microporosity combined with rigid polyamides are expected to provide good permeability and high permselectivity. Accordingly, a TB-derived diamine 2,8-diamino-4,10-dimethyl-6H,12H-5,11-methanodibenzo[1,5]-diazocine was synthesized according to a previous report (28). TB-based polyamides were successfully synthesized through a polycondensation reaction of TB diamine with four different diacids. The polymers have been well characterized, and their gas transport properties have been investigated.

2 Experimental section

2.1 Materials

4,4'-(Hexafluoroisopropylidene)bis(benzoic acid) (HFPA) (98%), isophthalic acid (98%), 2,6-naphthalenedicarboxylic acid (99%), 4,4'-oxy(benzoic acid) (99%), 2-methyl-4-nitroaniline (99%), trifluoroacetic acid, Pd/C, triphenyl phosphate (TPP) were purchased from Aldrich (USA). N, N-dimethylacetamide (DMAc), 1-methyl-2-pyrrolidine (NMP), pyridine, NaOH, and CaCl₂ were purchased from E. Merck, India. Methanol was purchased from SD Fine Chemicals, India. DMAc and NMP were dried using NaOH

and distilled from P₂O₅ before use. Pyridine was purified by distillation after being stirred with NaOH. 2,8-Diamino-4,10-dimethyl-6H,12H-5,11-methanodibenzo[1,5]-diazocine was prepared according to the reported procedure (28).

2.2 Characterization methods

The carbon, hydrogen and nitrogen contents of the compounds were analyzed by the pyrolysis method using a Vario EL (Elementar, Germany) elemental analyzer. The attenuated total reflection mode Fourier transform infrared (ATR-FTIR) spectra of the polymer membranes were recorded using a NEXUS Nicolet Impact-410 spectrophotometer. ¹H NMR spectra of the polymers were recorded using a Bruker 600 MHz instrument (Switzerland) by dissolving the desired quantity of the samples in different deuterated solvents, e.g. DMSO-*d*₆ or pyridine-*d*₅ at 30°C. The inherent viscosities (η_{inh}) of all the polymers were measured using an Ubbelohde viscometer at a polymer concentration of 0.5 g dl⁻¹ in DMAc at 30°C. The wide angle X-ray diffractometry (WAXD) of the polymers were conducted in reflection mode at room temperature using a Rigaku, Ultima III X-ray diffractometer. The Cu K α (0.154 nm) radiation source was used and a scanning range of 5–40° (2 θ) was employed with an intensity beam of 40 kV and 40 mA. The value of the amorphous peak maxima ($d_{spacing}$) was calculated utilizing Bragg's law ($d = n\lambda/2 \sin\theta$). TA instrument Q20 differential scanning calorimetry (DSC) was performed at a heating rate of 20°C/min to determine the glass transition temperature (T_g) of the polymer. The T_g of the polyamides were determined from the midpoint of the step transition in a second heat scan under a nitrogen atmosphere. A TA instruments TA Q50 instrument was used to perform the thermo gravimetric analysis (TGA) of the polymers. The polymer samples were dried at 160°C for 24 h under vacuum before performing TGA. The dried samples were heated from 50 to 800°C at a heating rate 10°C/min under synthetic air (N₂ : O₂ is 80 : 20). Mechanical properties of the membranes were measured using a Universal Testing Machine UTM H5KS Tinius Olsen, equipped with 50 N load cell and a strain rate of 5% min⁻¹ of the specimen length at 30°C. Rectangular specimens of 10 mm width, with an effective length of 25 mm (distance between the clamps) and a thickness of around 63–77 μ m were used for the measurement. At least four specimens of each sample were used for each measurement, and the average values were reported. The dielectric constant (ϵ) values were calculated using a HIOKI 3532-50 LCR Hi Tester. The capacitance values of the polymer membranes were

measured using the parallel plate capacitor method, at 1 MHz at 30°C and relative humidity 45. The densities (ρ) of the PA membranes were determined by Archimedes' principle using a Wallace High Precision Densimeter-X22B (UK) at 30°C. The samples were sequentially weighed in air and high purity isooctane at 30°C. The fractional free volumes (FFV) of the polymers were determined by the following equation [1]:

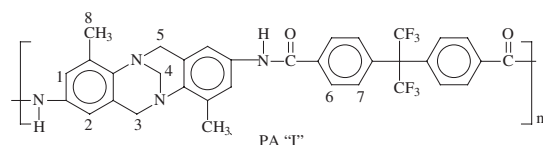
$$\text{FFV} = (V - 1.3 V_w) / V \quad [1]$$

where, V is the specific volume ($V = 1/\rho$) of the polymer determined from the measured density. The van der Waals volume (V_w) was estimated by the Hyperchem computer program, version 8.0 (29).

2.3 Synthesis of TB-based polyamides

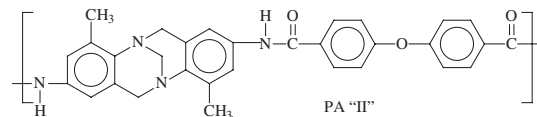
The polyamides (PA "I"–"IV") were synthesized by the polycondensation reaction of an equimolar amount of the Troeger base-bridged diamine with four different aromatic diacids, using NMP as a solvent and in the presence of TPP and pyridine as a condensing agent. As a representative, the polymerization of one of the polyamide PA "I" is described here. A three-neck round bottom flask equipped with a nitrogen inlet and a refluxed condenser was charged with 0.44 g TB (1.57 mmol), 0.616 g HFPA (1.57 mmol) and 0.36 g calcium chloride. To that flask 5 ml NMP, 1.4 ml pyridine and 1.4 ml triphenyl phosphate (TPP) (5.34 mmol) were added. The mixture was heated to 110°C for 6 h under constant stirring. The highly viscous reaction mixture was cooled to room temperature and slowly added to 300 ml methanol with constant stirring. A fiber like precipitate was obtained. The white fibrous polymer was filtered and washed with methanol followed by distilled water (hot and cold) to remove any adsorbed solvent and CaCl_2 . The polymer was dried overnight at 120°C under vacuum; then PAs were prepared by a similar polyamidation reaction of TB with three other dicarboxylic acids.

The analytical details of the polymers are given below:

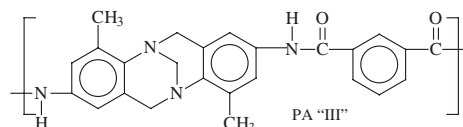


Anal. calcd for $\text{C}_{34}\text{H}_{26}\text{F}_6\text{N}_4\text{O}_2$ (636.59 g mol⁻¹): C, 64.15%; H, 4.12%; N 8.80%; O 5.03%; F, 17.91%. %; found: C, 64.21%; H, 4.14%; N 8.84%; O 5.01%; F, 17.87%. FTIR (KBr, cm⁻¹): 3302 (N-H stretching), 2947 (aromatic C-H stretching), 1656

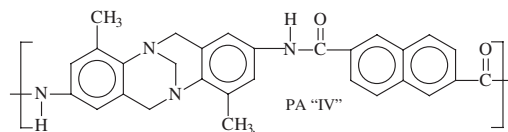
(>C=O stretching). ¹H-NMR: $\delta_{\text{H(ppm)}}$ (600 MHz; pyridine-d₅; Me₄Si): 11.06 (s, 2H, amide protons), 8.28 (d, $J = 7.8$ Hz, 4H, H⁶), 7.76 (m, 4H, H¹, H²), 7.51 (d, $J = 7.2$ Hz, 4H, H⁷), 4.59 (d, $J = 12$ Hz, 2H, H³), 4.31 (s, 2H, H⁴), 4.15 (d, $J = 12$ Hz, 2H, H⁵), 2.43 (s, 6H, H⁸).



Anal. calcd for $\text{C}_{31}\text{H}_{26}\text{N}_4\text{O}_3$ (502.56 g mol⁻¹): C, 74.09%; H, 5.21%; N 11.15%; O 9.55%. %; found: C, 74.03%; H, 5.26%; N 11.13%; O 9.57%. FTIR (KBr, cm⁻¹): 3286 (N-H stretching), 2946 (aromatic C-H stretching), 1637 (>C=O stretching).



Anal. calcd for $\text{C}_{25}\text{H}_{22}\text{N}_4\text{O}_2$ (410.47 g mol⁻¹): C, 73.15%; H, 5.40%; N 13.65%; O 7.80%. %; found: C, 73.17%; H, 5.36%; N 13.66%; O 7.85%. FTIR (KBr, cm⁻¹): 3295 (N-H stretching), 2938 (aromatic C-H stretching), 1653 (>C=O stretching).



Anal. calcd for $\text{C}_{29}\text{H}_{24}\text{N}_4\text{O}_2$ (460.53 g mol⁻¹): C, 75.63%; H, 5.25%; N 12.17%; O 6.95%. %; found: C, 75.60%; H, 5.23%; N 12.21%; O 6.98%. FTIR (KBr, cm⁻¹): 3286 (N-H stretching), 2943 (aromatic C-H stretching), 1645 (>C=O stretching).

2.4 Membrane fabrication

PA membranes were prepared by solution casting. The homogenous polymer solution was prepared by dissolving the polymers in DMAc at a concentration of 10% (w/v). The polymer solutions were filtered and poured into Petri dishes. The Petri dishes were placed in an oven at 80°C overnight, followed by slow heating to 150°C and kept for 6 h to remove most of the solvent. The membranes were further vacuum dried at 150°C for 48 h. The membranes were removed from the Petri dishes by immersing them in boiling water. The membranes obtained were dried under vacuum at 120°C for 8 h to remove any absorbed moisture. The thickness of the membranes ranged from 63 to 77 μm .

2.5 Gas permeation measurements

The gas permeability of the PA membranes were investigated using permeation test system PTS 50F-16M manufactured by Indian High Vacuum Pumps (India). The membranes were degassed in the permeation cell under high vacuum at 35°C for at least 24 h. The pure gases (excel grade) were pressurized (3.5 bar) on the membrane in the following order to avoid plasticization: CH₄, N₂, O₂ and CO₂. Gas permeability coefficient (P), diffusion coefficients (D), solubility coefficients (S), ideal diffusibility selectivity (α_D) and ideal solubility selectivity (α_S) were calculated according to the reported procedure (4, 10).

3 Results and discussion

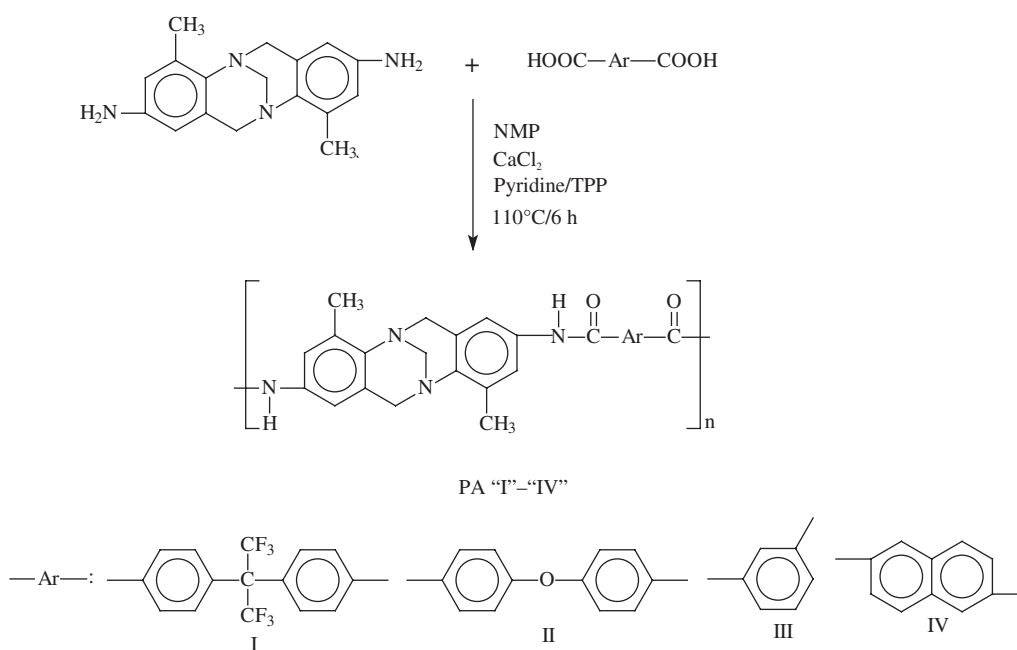
3.1 Synthesis of polymers

A series of new aromatic polyamides PA “I”–“IV” were prepared by phosphorylation polyamidation reaction of TB with different commercial diacids using TPP and pyridine as condensing agent as shown in Scheme 1 (30). The polymerization yield was nearly quantitative. The inherent viscosity (Table 1) of the polymers in DMAc ranged from 0.85 to 1.13 dl/g. Membranes prepared from solution casting were tough and flexible. The elemental (C, H, N) composition of the polymers were checked by the

pyrolysis method and were in good agreement with the calculated values from the polymer repeat unit structures. The formation of the polymers were confirmed by FTIR-ATR and ¹H NMR spectroscopic methods. The FTIR-ATR spectra of these polymers exhibited the characteristic absorptions bands at 3280–3320 and 1636–1659 cm⁻¹ that correspond to characteristics >N-H and >C=O stretching (31). The structures of the PA “I” were also verified by ¹H NMR spectra (Figure 1). The peaks appeared at 11.06 ppm corresponds to the amide proton that supports the formation of the amide linkages. All the polyamides are soluble in polar aprotic solvents, such as NMP, DMAc and DMF, at room temperature. However, except PA “I” (containing 6F group), other polymers showed poor solubility in pyridine solvents, due to the strong inter chain interactions and efficient packing of the polymer chains of amide linkages.

3.2 Molecular packing

WAXD diffraction patterns were measured to investigate the polymers chain packing. Figure 2 represents the WAXD diffraction patterns of the polyamides and the packing parameters of WAXD are summarized in Table 1. The broad spectra suggests the amorphous nature of the polyamides. The center of the broad peak in the diffraction pattern of WAXD was used to calculate average intersegmental spacing or d_{spacing} between the chains, calculated by Bragg's equation (16, 32). All PA membranes



Scheme 1: Synthesis of the polyamides (PA “I”–“IV”).

Table 1: Physical properties and packing parameters of the polyamides.

Polymer	η_{inh} (dl/g) ^a	Density ^b	2θ (°) ^c	d_{sp} (Å) ^d	V_w (cm ³ mol ⁻¹) ^e	FFV ^f
PA "I"	0.85	1.10	16.4	5.3	333	0.245
PA "II"	1.07	1.07	19.1	4.6	278	0.229
PA "III"	1.04	1.14	20.1	4.4	228	0.168
PA "IV"	1.13	1.15	20.0	4.4	255	0.166

^a η_{inh} , Inherent viscosity at 30°C. ^bDensity (g cm⁻³) measured at 30°C.^c 2θ , Diffraction position. ^d d_{sp} , Intersegmental distance between the polymer chain obtained from the Bragg equation. ^e V_w , Van der Waals volume. ^fFFV, The FFV values of the PAs determined experimentally.

had two broad diffraction peaks, ranging from low angel side to high angel side. For PA "I", PA "III" and PA "IV" peaks located at low angel $2\theta = 16.7^\circ$, 19.7° and 19.8° can be assigned to the main inter chain distance in the amorphous domain. The peaks located at the high angel side $2\theta = 22.6^\circ$, 24.6° and 25.7° can be assigned to the π - π stacking of aromatic rings or the interchain distance in the ordered domain or the loose stacks in the polymer chains. PA "II" showed only a broad amorphous halo peak in WAXD at $2\theta = 19.1^\circ$, representing typical amorphous morphology (33). Different diffraction patterns in WAXD provides an idea of free volume distribution and morphologies apart from the free volume. Different free volume morphologies arise from the structural differences of the PAs which attributed different gas permeability (34).

3.3 Thermal properties

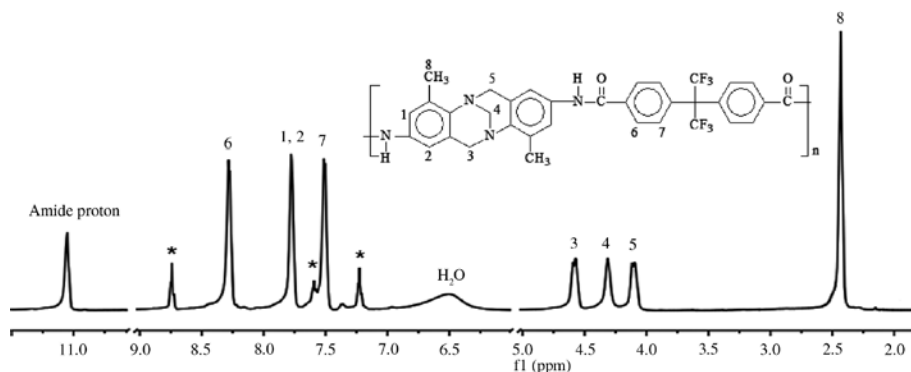
The glass transition temperature (T_g) of the polymers (Table 2) were found to be in the range of 283–290°C, depending on the diacid components (Figure 3). The T_g values were according to the decreasing order of stiffness

of the polymer chains. The lowest T_g was observed for the PA derived from the diacid with flexible isopropylidene units (6F). The polymers with rigid substituents restricted the free rotation of the polymer chain and showed a higher T_g compared to that of the other polymers. The rigid naphthalene containing polymer backbone exhibited the highest T_g value (290°C). The thermal stabilities of the polymers were evaluated by thermogravimetric analysis (TGA) in an air atmosphere (Figure 4). Their decomposition temperatures (10% weight loss) for the PAs were in the range of 343–431°C, and the maximum decomposition temperatures were in the range of 431°C.

The mechanical properties of the PA membranes are listed in Table 2. The membranes showed a tensile strength in the range of 66–95 MPa, an elongation at break in the range of 5.5–7.9% and a tensile modulus in the range of 1.9–2.6 GPa.

3.4 Gas permeation properties

The gas permeability of the PA membranes was tested for four gases CH₄, N₂, O₂ and CO₂ at 35°C with a feed pressure of 3.5 bar. The gas permeability coefficients (P) and ideal selectivities (α) are shown in Table 3. p-Values were measured from the steady-state region of the downstream pressure-time curve by using the constant-volume/variable-pressure technique. The order of gas permeabilities for all PA membranes follow the following order: $P(\text{CO}_2) > P(\text{O}_2) > P(\text{N}_2) > P(\text{CH}_4)$. This order is the reverse order of their kinetic diameters (σ) of the gases (Å): 3.3 for CO₂, 3.46 for O₂, 3.64 for N₂ and 3.8 for CH₄, representing that the gas permeabilities decrease with the increase of kinetic diameter of gases, and the same trend was observed in other glassy polymers (36). For each gases, the gas permeability increases in the order of PA "IV" < PA "III" < PA "II" < PA "I". The CO₂ permeability of the membranes were in the range

**Figure 1:** ¹H-NMR spectrum of PA "I" in pyridine-*d*₅ (*signals at 8.74, 7.59, and 7.22 ppm are for pyridine).

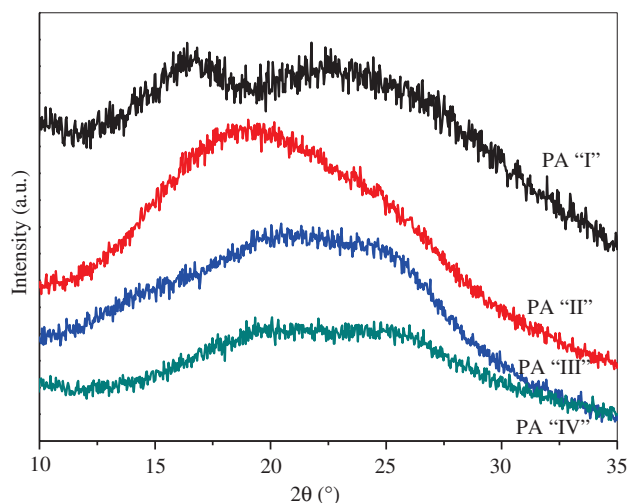


Figure 2: WAXD diffraction curves of the polyamide membranes.

Table 2: Thermal, mechanical and electrical properties of the polyamides.

Polymer	T_g (°C) ^a	T_d (°C) ^b	T.S. (MPa) ^c	Modulus (GPa) ^d	Elongation at break (%) ^e	ϵ'
PA "I"	283	431	66	1.93	5.5	2.07
PA "II"	284	356	79	2.17	5.7	2.17
PA "III"	285	365	69	2.19	6.7	2.39
PA "IV"	290	351	90	2.6	7.9	2.29

^aGlass transition temperature determined by DSC, heating rate at 20°C/min. ^b10% Degradation temperature was measured by TGA under air, heating rate at 10°C/min. ^cTensile strength. ^dYoung's modulus. ^ePercent of elongation at break. ^fDielectric constant (ϵ) at 1 MHz frequency and 30°C temperature.

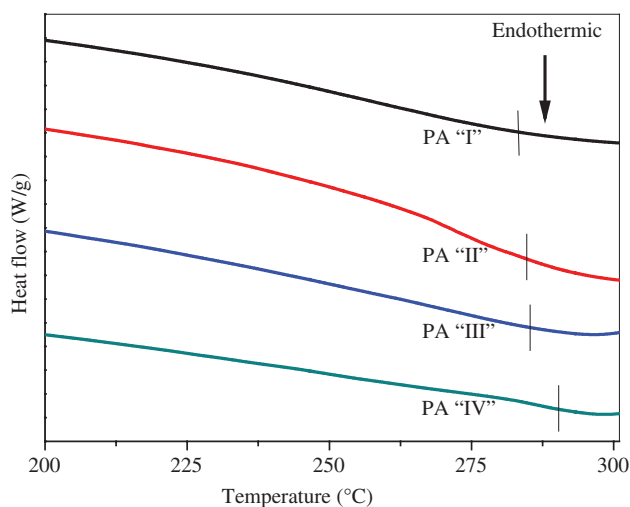


Figure 3: DSC curves (2nd heat scan) of the polymers (heating rate: 20°C min⁻¹).

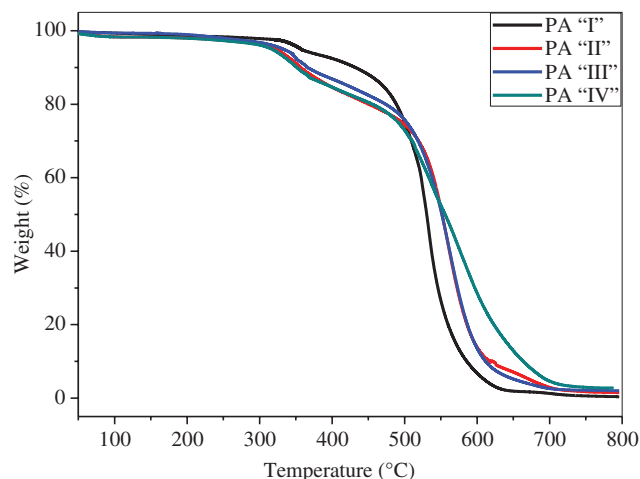
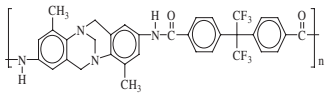
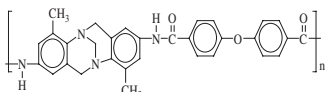
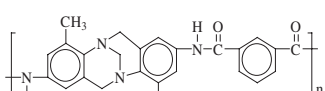
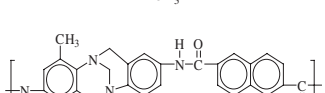
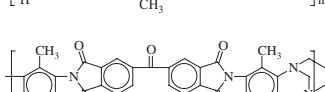
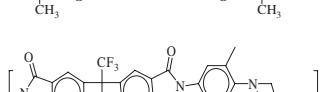
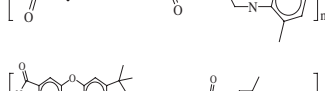
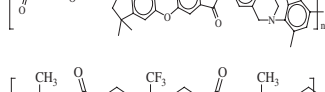
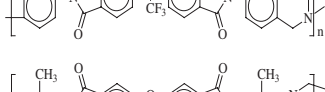
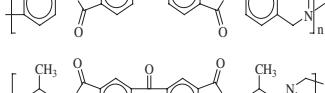
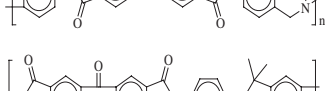
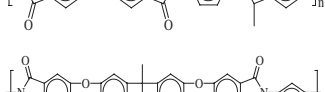
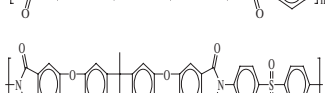
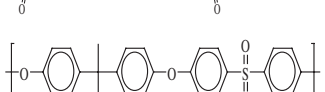


Figure 4: TGA thermograms of the polymers in air (heating rate: 10°C min⁻¹).

of 86–109 Barrer. These values are much higher than commercial polyimide Matrimid® ($P_{CO_2} = 8.7$). The methyl groups present in the TB unit of the polymer help to increase the distance between the polymer chains and to increase the permeability (18). Gas permeability of the membranes strongly depends on average interchain spacing ($d_{spacing}$) and FFV as can be seen from Table 3. Chemical structures of the polymer have a significant influence on permeability. PA "I" containing large bulky 6F groups exhibited a relatively higher permeability. Interchain spacing is used to measure the openness of the polymer backbone, i.e. FFV and is comparative to the permeability. The presence of TB units in polymer backbone improves the permeability, compared to the analogous 6F group (same acid part HFPA) containing polymer membranes like PA 9B and PA "S2" (37, 38). The permeability of PA "II" is greater than those PA "III" and PA "IV", due to the incorporation of flexibility into the polymer chain through ether linkages. The PA "III" showed higher permeability than PA "IV" due to the unsymmetrical structure of the acid moiety, except CO_2 gas. The PA "IV" exhibited lowest permeability for all the gases due to higher chain packing density, as evident from its FFV and $d_{spacing}$ values (Table 1). For amorphous polymer systems, the gas permeability can be approximately correlated with FFV by the following equation $P = Ae^{(-B/FFV)}$ where, the parameters A and B characteristic of each gas (10, 11). The PAs in the present investigation also satisfactory follow the same trend (Figure 5). According to the free volume theory, the higher is the free volume in polymer matrix the higher will be the available space for a gas molecule to diffuse. FFV and diffusivity both increases by the introduction of side methyl groups in m-position of the amide bond. This group hinders

Table 3: Gas permeability coefficients (P) in Barrer and permselectivities (α) of the polyamides, at 35°C, 3.5 bar (data from film aged for 10 days) and their comparison with other commercially available and reported polymers.

Polymer	Polymer structure	P(CO ₂)	P(O ₂)	P(N ₂)	P(CH ₄)	α (CO ₂ /CH ₄)	α (O ₂ /N ₂)	Ref.
PA "I"		109.1	21.6	2.87	2.17	50.3	7.52	^a
PA "II"		92.2	18.3	2.54	1.97	46.8	7.20	^a
PA "III"		84.7	16.8	2.33	1.75	48.4	7.21	^a
PA "IV"		86.4	14.1	2.16	1.61	53.7	6.52	^a
PI-TB-2		55.0	14.0	2.50	2.10	26.0	5.48	(16) ^b
TBDA1-6FDA-PI		155	28.0	6.50	3.30	46.9	3.90	(20) ^c
TBDA1-SBI-PI		895	190	350	45.0	19.7	5.40	(24) ^d
PI-TB-3		218	42.0	9.50	6.70	32.7	4.50	(25) ^e
PI-TB-4		13.5	3.50	1.30	1.00	13.5	2.80	(25) ^e
PI-TB-5		19.6	4.90	1.90	1.70	11.5	2.60	(25) ^e
Matrimi-d®		8.70	1.90	0.27	0.24	36.0	7.00	(35)
Ultem®		1.33	0.41	0.05	0.03	36.90	8.00	(4)
Extrem®		3.28	0.81	0.13	0.13	25.20	6.20	(4)
Polysulf-one		5.6	1.2	0.18	0.18	22.0	6.00	(4)

Gas permeability coefficient (P) in Barrer. 1 Barrer = 10⁻¹⁰ cm³ (STP) cm/cm² s cm Hg.^aThis study. ^bMeasured at 1 atm, 35°C. ^cMeasured at 1 bar, 35°C. ^dMeasured at 1 bar, 35°C. ^eMeasured at 1 atm, 35°C.

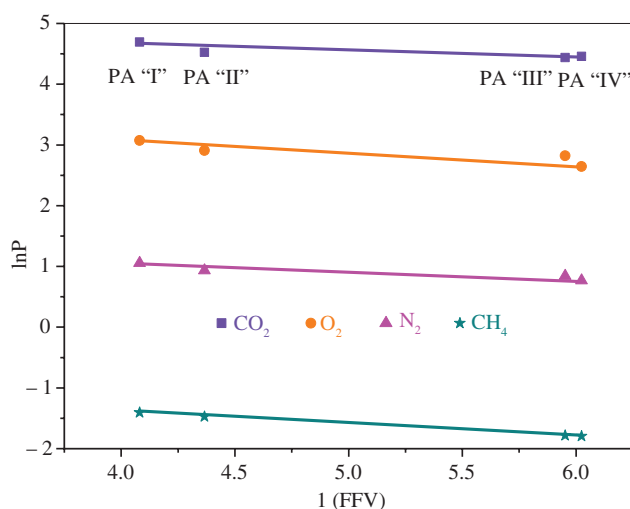


Figure 5: The dependence of gas permeability vs. reciprocal of fractional free volume of polyamides for CO_2 , O_2 , N_2 and CH_4 gases.

the rotation of the polymer chains that causes less efficient chain packing in the polymer matrix. Despite having very high FFV of PA I, the gas permeability of this polymer was considerably lower than many other PIMs, e.g. TBDA1-SBI-PI (Table 3) (24). However, gas permeability depends on many factors, e.g. type of PIMs, membrane preparation technique, measurement technique, and applied pressure and temperature.

The relative order of diffusion coefficient follows the trend: $D(\text{O}_2) > D(\text{CO}_2) > D(\text{N}_2) > D(\text{CH}_4)$. $D(\text{O}_2) > D(\text{CO}_2)$ cannot be explained by the kinetic diameter values of these two gases. However, this trend is in order of effective molecular diameter (d_{ef}) of the gas molecules as reported by Teplyakov and Mears (39). As d_{ef} of O_2 (3.02 Å) is higher than CO_2 (2.89 Å), the diffusion coefficient of O_2 is higher. From Table 4, it is observed that the D values for every gases through the polymer membranes follow the order PA "I" > PA "II" > PA "III" > PA "IV".

Solubility coefficient of the studied gases follow the order $S(\text{CO}_2) > S(\text{O}_2) > S(\text{N}_2) > S(\text{CH}_4)$. The solubility of gases in a membrane is related to their critical

temperatures (T_c), as condensability depends on T_c . Higher solubility of CO_2 into the polymer membranes reflected from the T_c (31.04°C) compares to other gases [T_c CH_4 , N_2 , O_2 = -82.3, -146.9, -118.6°C]. The TB unit in the polymer backbone may account for the enhanced solubility of CO_2 . TB contains two extra polar nitrogens (tertiary amine) that could interact strongly by Lewis acid-base interaction with CO_2 molecules having a strong quadrupole moment (20). The polar character of the amide bond also influenced the solubility coefficient (12). Analysis of the data in Table 4 shows that permeability differences in the PA membranes mainly comes from solubility coefficient values, rather than diffusion coefficients. The presence of the polar group in the polymer chain enhances intermolecular interactions, results in a high solubility coefficient.

Analysis of the data presented in Table 3 exhibits great improvements in gas separation results, in particular, for the gas pair CO_2/CH_4 and O_2/N_2 . The PAs showed improved selectivity as compared to the commercial Matrimid® membrane (35). The ideal gas selectivity follows the following order PA "II" < PA "III" < PA "I" < PA "IV". Except the membrane PA "I", the "trade-off" relationships between P and α follows the same order. The presence of 6F group in PA "I" restricted the segmental motion more, which in turn increases the selectivity. The selectivity coefficients of CO_2/CH_4 and O_2/N_2 were in the range of 48.4–53.6 and 6.5–7.5. High selectivity for CO_2/CH_4 and O_2/N_2 gas pairs were due to amide bonds which introduce intramolecular rigidity by densifying the polymer chain (12).

Diffusivity and solubility coefficients for the PAs are shown in Table 4. As expected, compared to diffusivity values, solubility values are much higher. The gas diffusivity selectivities of uncondensable gas pairs (O_2/N_2) of PAs were in the range of 3.6–4.8, and its solubility.

Selectivities were in the range of 1.5–1.8. So, judging from the result for O_2/N_2 gas pairs permselectivity values, the main contribution factor could be diffusivity selectivity, as O_2 and N_2 gas molecule has less affinity with the polymer matrix. The increased selectivity of PA "IV" could be due to the restricted segmental motions. The

Table 4: Gas diffusion coefficients, D ($10^{-8} \text{ cm}^2/\text{s}$), solubility coefficients (S) in ($10^{-2} \text{ cm}^3 (\text{STP})/(\text{cm}^3 \text{ cm Hg})$), diffusivity selectivity (α_D) and solubility selectivity (α_S) values of the polyamides.

Polymer	CO_2		O_2		N_2		CH_4		CO_2/CH_4		O_2/N_2	
	D	S	D	S	D	S	D	S	α_D	α_S	α_D	α_S
PA "I"	7.2	15.1	8.78	2.46	1.8	1.59	1.61	1.34	4.47	11.26	4.87	1.54
PA "II"	6.63	13.9	8.09	2.26	1.67	1.52	1.62	1.21	4.09	11.48	4.84	1.48
PA "III"	7.0	12.1	8.70	1.93	1.83	1.27	1.56	1.12	4.48	10.80	4.75	1.51
PA "IV"	6.69	12.9	6.77	2.08	1.86	1.16	1.51	1.06	4.43	12.16	3.69	1.79

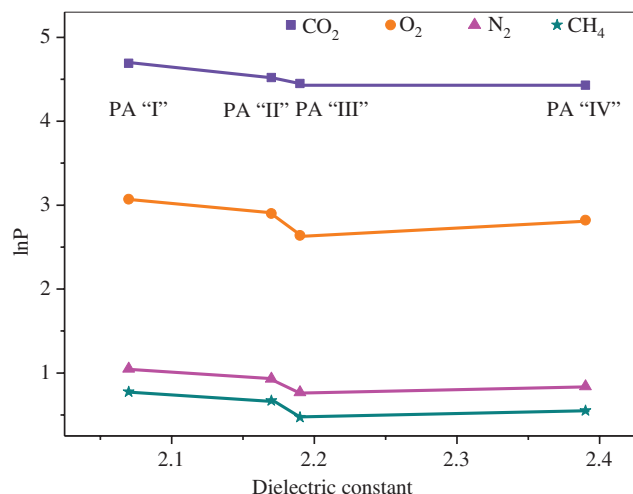


Figure 6: The dependence of gas permeability vs. dielectric constant of the polyamide membranes for CO_2 , O_2 , N_2 and CH_4 gases.

gas diffusivity selectivities of (CO_2/CH_4) gas pairs of PAs were in the range of 4.09–4.48, and the solubility selectivities were in the range of 10.8–12.1. The analysis of the data reveals that permselectivity of (CO_2/CH_4) has mainly originated from solubility selectivities, as CO_2 has a strong interaction with the polymer matrix. The increment of the separation performances of (O_2/N_2) gas pairs indicates that separation of this gas pair depends on size selectivity based principle as they have small differences in kinetic diameters between the gas molecules.

Introduction of TB units into the polymer matrix significantly increases in selectivity with moderate permeability. The PAs under this investigation showed a decrease in permeability for all gases in comparison to the TB-bridged polyimides reported by Jin et al. (20). However, the present PAs showed an increase in selectivity for CO_2/CH_4 and O_2/N_2 gas pairs. According to Jian et al. permeability of TB polymers mostly comes from solubility (S), as it is directly related to the polymer structure (22). The experimental data from Table 4 also indicate the same result. In CO_2/CH_4 separation, solubility selectivity mainly dominated due to the Lewis acid-base interaction between the CO_2 molecule and the TB unit. McKeown et al. also reported the same behavior for the TB polymer. They described selectivity being primarily due to the much higher solubility of CO_2 (solubility selectivity) rather than selectivity based on diffusivity (21).

Matsumoto et al. (40) and Miyata et al. (41) reported a linear relationship between the dielectric constant (ϵ) and CO_2 and CH_4 permeabilities for several polymers. Miyata et al. also showed a linear relationship between permeability and the diffusion coefficient with ϵ in 6FDA based polyimides (41). The PAs under this investigation showed a linear relationship between P and ϵ (Figure 6). From the

Table 4, it can be seen that the ϵ of the PAs varied from 2.07 to 2.39 in 1 MHz. The order of ϵ was PA "I" < PA "II" < PA "III" < PA "IV". PA "I" containing [$>\text{C}(\text{CF}_3)$] showed the lowest ϵ value due to highest fluorine content (13).

3.5 Comparison with other commercially available polymers and previously reported polymer membranes

The gas separation performance of the PAs is plotted graphically in Figures 7 and 8, respectively. In the graph,

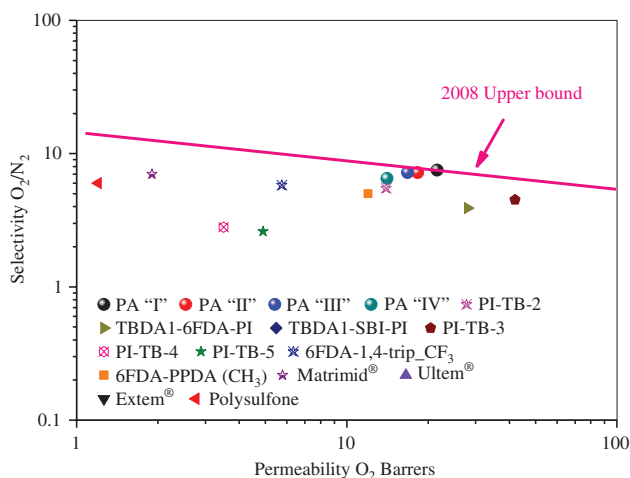


Figure 7: Relationship between gas permeability (P) and gas pairs selectivity (α) for O_2/N_2 separation in Robeson upper bound plots. Data points of structurally similar polymers and other commercially available polymers also reported.

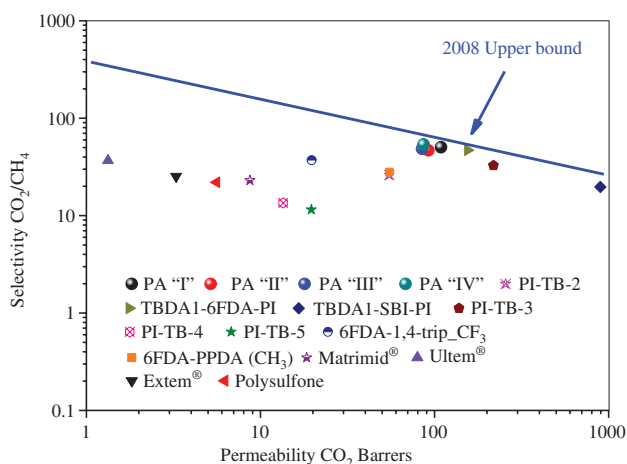


Figure 8: Relationship between gas permeability (P) and gas pairs selectivity (α) for CO_2/CH_4 separation in Robeson upper bound plots. Data points of structurally similar polymers and other commercially available polymers also reported.

permselectivity for the important gas pairs, CO_2/CH_4 , O_2/N_2 plotted as ordinate, and $\text{P}(\text{CO}_2)$, $\text{P}(\text{O}_2)$ plotted as abscissa. The solid line in the graph represents the Robeson's 2008 upper bound. In the permeability-selectivity plots, the data points for all the PAs in this study along with some recently reported structurally similar polymers (16, 20, 24, 25, 42) and a few typical commercial membranes (e.g. Matrimid®, Ultem®, Extem® and Polysulfone) are included for better comparison. These plots can be used as a universal performance indicator for the separation of two gases. It can be seen from these plots that the PAs in this investigation showed an improvement in gas separation performance compared to many commercial reported polymers. The results further indicate that methyl substitution and amide bonds in the polymer backbone effectively improved the selectivity of the resulting polymer membranes (25). The performance of these membranes for gas separation properties fall in the attractive region of Robeson's upper bound. The permeability/selectivity trade-off data of the membrane for the gas pairs exceed those conventional polymers, and outperformed other reported polymers (24).

4 Conclusions

A series of new TB-bridged PAs has been designed and synthesized. A general method is reported for the synthesis of conventional PAs using diamine and with four different diacids. The membranes were prepared by the solution casting method and tested for gas permeability measurements. In general, the TB unit in the PAs backbone enhances the gas permeability and in particular, increases the permselectivity of CO_2/CH_4 and O_2/N_2 gas pairs. Systematic investigation and analyses of the correlation between molecular packing and properties of the PAs match nicely with the gas permeation results. The pure gas selectivity has improved up to 53 for CO_2/CH_4 gas pairs. The PAs provides notable data points regarding the position about the Robeson upper bound. This straightforward and efficient strategy may be readily applied toward preparing of a technologically competitive polymer membrane for CO_2 productivity with low cost and high energy efficiency.

Acknowledgments: S. Bisoi acknowledges the University Grant Commission, New Delhi, India, for providing his research fellowship to carry out this work. The financial support from the Department of Science and Technology (DST), India (Grant No. SR/S3/ME/0008/2010) is gratefully acknowledged.

References

1. Wang S, Li X, Wu H, Tian Z, Xin Q, He G, Peng D, Chen S, Yin Y, Jiang Z, Guiver MD. Advances in high permeability polymer-based membrane materials for CO_2 separations. *Energy Environ Sci.* 2016;9(6):1863–90.
2. Baker RW, Low BT. Gas separation membrane materials: a perspective. *Macromolecules.* 2014;47(20):6999–7013.
3. Yampolskii Y. Polymeric gas separation membranes. *Macromolecules.* 2012;45(8):3298–311.
4. Bisoi S, Mandal AK, Padmanabhan V, Banerjee S. Aromatic polyamides containing trityl substituted triphenylamine: gas transport properties and molecular dynamics simulations. *J Memb Sci.* 2017;522:77–90.
5. Budd PM, McKeown NB. Highly permeable polymers for gas separation membranes. *Polym Chem.* 2010;1(1):63–8.
6. Maier G. Gas separation by polymer membranes: beyond the border. *Angew Chem Int Ed Engl.* 2013;52(19):4982–4.
7. Robeson LM. The upper bound revisited. *J Memb Sci.* 2008;320(1–2):390–400.
8. Du N, Park HB, Dal-Cin MM, Guiver MD. Advances in high permeability polymeric membrane materials for CO_2 separations. *Energy Environ Sci.* 2012;5(6):7306–22.
9. Xiao Y, Low BT, Hosseini SS, Chung TS, Paul DR. The strategies of molecular architecture and modification of polyimide-based membranes for CO_2 removal from natural gas – a review. *Prog Polym Sci.* 2009;34(6):561–80.
10. Bera D, Padmanabhan V, Banerjee S. Highly gas permeable polyamides based on substituted triphenylamine. *Macromolecules.* 2015;48(13):4541–54.
11. Bisoi S, Bandyopadhyay P, Bera D, Banerjee S. Effect of bulky groups on gas transport properties of semifluorinated poly(ether amide)s containing pyridine moiety. *Eur Polym J.* 2015;66:419–28.
12. Espeso J, Lozano AE, de la Campa JG, de Abajo J. Effect of substituents on the permeation properties of polyamide membranes. *J Memb Sci.* 2006;280(1–2):659–65.
13. Banerjee S. Handbook of specialty fluorinated polymers: Preparation, Properties, and Applications. Elsevier, USA, 2015.
14. Preparation of solution-processable colorless polyamide-imides with extremely low thermal expansion coefficients through an in-situ silylation method for potential space optical applications [Internet]. *e-Polymers.* 2016;16:395. Available from: <http://www.degruyter.com/view/j/epoly.2016.16.issue-5/epoly-2016-0100/epoly-2016-0100.xml>.
15. Carta M, Bernardo P, Clarizia G, Jansen JC, McKeown NB. Gas Permeability of hexaphenylbenzene based polymers of intrinsic microporosity. *Macromolecules.* 2014;47(23):8320–7.
16. Zhuang Y, Seong JG, Do YS, Jo HJ, Cui Z, Lee J, Lee YM, Guiver MD. Intrinsically microporous soluble polyimides incorporating tröger's base for membrane gas separation. *Macromolecules.* 2014;47(10):3254–62.
17. Zhang J, Kang H, Martin J, Zhang S, Thomas S, Merkel TC, Jin J. The enhancement of chain rigidity and gas transport performance of polymers of intrinsic microporosity via intramolecular locking of the spiro-carbon. *Chem Commun.* 2016;52(39):6553–6.
18. Carta M, Croad M, Malpass-Evans R, Jansen JC, Bernardo P, Clarizia G, Friess K, Lanč M, McKeown NB. Triptycene induced

- enhancement of membrane gas selectivity for microporous Tröger's base polymers. *Adv Mater.* 2014;26(21):3526–31.
19. Luo S, Wiegand JR, Kazanowska B, Doherty CM, Konstas K, Hill AJ, Guo R. Finely tuning the free volume architecture in iptycene-containing polyimides for highly selective and fast hydrogen transport. *Macromolecules.* 2016;49(9):3395–405.
 20. Wang Z, Wang D, Zhang F, Jin J. Tröger's base-based microporous polyimide membranes for high-performance gas separation. *ACS Macro Lett.* 2014;3(7):597–601.
 21. Carta M, Malpass-Evans R, Croad M, Rogan Y, Jansen JC, Bernardo P, Bazzarelli F, McKeown NB. An efficient polymer molecular sieve for membrane gas separations. *Science.* 2013;339(6117):303–7.
 22. Wang ZG, Liu X, Wang D, Jin J. Tröger's base-based copolymers with intrinsic microporosity for CO₂ separation and effect of Tröger's base on separation performance. *Polym Chem.* 2014;5:2793.
 23. Rogan Y, Malpass-Evans R, Carta M, Lee M, Jansen JC, Bernardo P, Clarizia G, Tocci E, Friess K, Lanč M, McKeown NB. A highly permeable polyimide with enhanced selectivity for membrane gas separations. *J Mater Chem A.* 2014;2(14):4874–7.
 24. Wang Z, Wang D, Jin J. Microporous polyimides with rationally designed chain structure achieving high performance for gas separation. *Macromolecules.* 2014;47(21):7477–83.
 25. Zhuang Y, Seong JG, Do YS, Lee WH, Lee MJ, Guiver MD, Lee YM. High-strength, soluble polyimide membranes incorporating Tröger's Base for gas separation. *J Memb Sci.* 2016;504:55–65.
 26. Seong JG, Zhuang Y, Kim S, Do YS, Lee WH, Guiver MD, Lee YM. Effect of methanol treatment on gas sorption and transport behavior of intrinsically microporous polyimide membranes incorporating Tröger's base. *J Memb Sci.* 2015;480:104–14.
 27. Lee M, Bezzu CG, Carta M, Bernardo P, Clarizia G, Jansen JC, McKeown NB. Enhancing the gas permeability of Tröger's base derived polyimides of intrinsic microporosity. *Macromolecules.* 2016;49(11):4147–54.
 28. Kiehne U, Weilandt T, Lützen A. Diastereoselective self-assembly of double-stranded helicates from Tröger's base derivatives. *Org Lett.* 2007;9(7):1283–6.
 29. HyperChem(TM) Professional 7.51, Hypercube, Inc., 1115 NW 4th Street, Gainesville, Florida 32601, USA [Internet]. Available from: <http://www.hyper.com/Default.aspx?tabid=373>.
 30. Mondal S, Das N. Triptycene based organosoluble polyamides: synthesis, characterization and study of the effect of chain flexibility on morphology. *RSC Adv.* 2014;4:61383–93.
 31. Maji S, Banerjee S. Synthesis, characterization, and properties of novel fluorine containing aromatic polyamides. *J Appl Polym Sci.* 2008;108(2):1356–64.
 32. Calle M, Jo HJ, Doherty CM, Hill AJ, Lee YM. Cross-linked thermally rearranged poly(benzoxazole-co-imide) membranes prepared from ortho-hydroxycopolyimides containing pendant carboxyl groups and gas separation properties. *Macromolecules.* 2015;48(8):2603–13.
 33. Kumbharkar SC, Karadkar PB, Kharul UK. Enhancement of gas permeation properties of polybenzimidazoles by systematic structure architecture. *J Memb Sci.* 2006;286(1–2):161–9.
 34. Xu JW, Chng ML, Chung TS, He CB, Wang R. Permeability of polyimides derived from non-coplanar diamines and 4,4'-(hexafluoroisopropylidene)diphthalic anhydride. *Polymer (Guildf).* 2003;44(16):4715–21.
 35. Guiver MD, Robertson GP, Dai Y, Bilodeau F, Kang YS, Lee KJ, Jho JY, Won J. Structural characterization and gas-transport properties of brominated matrimid polyimide. *J Polym Sci Part A Polym Chem.* 2002;40(23):4193–204.
 36. Bandyopadhyay P, Bera D, Ghosh S, Banerjee S. Synthesis, characterization and gas transport properties of cardo bis(phenylphenyl)fluorene based semifluorinated poly(ether amide)s. *RSC Adv.* 2014;4(53):28078–92.
 37. Bera D, Bandyopadhyay P, Ghosh S, Banerjee S. Gas transport properties of aromatic polyamides containing adamantyl moiety. *J Memb Sci.* 2014;453:175–91.
 38. Bandyopadhyay P, Banerjee S. Spiro[fluorene-9,9'-xanthene] containing fluorinated poly(ether amide)s: synthesis, characterization and gas transport properties. *Eur Polym J.* 2015;69:140–55.
 39. Mason CR, Maynard-Atem L, Al-Harbi NM, Budd PM, Bernardo P, Bazzarelli F, Clarizia G, Jansen JC. Polymer of intrinsic microporosity incorporating thioamide functionality: preparation and gas transport properties. *Macromolecules.* 2011;44(16):6471–9.
 40. Matsumoto K, Xu P, Nishikimi T. Gas permeation of aromatic polyimides. I. Relationship between gas permeabilities and dielectric constants. *J Memb Sci.* 1993;81(1):15–22.
 41. Miyata S, Sato S, Nagai K, Nakagawa T, Kudo K. Relationship between gas transport properties and fractional free volume determined from dielectric constant in polyimide films containing the hexafluoroisopropylidene group. *J Appl Polym Sci.* 2008;107(6):3933–44.
 42. Wiegand JR, Smith ZP, Liu Q, Patterson CT, Freeman BD, Guo R. Synthesis and characterization of triptycene-based polyimides with tunable high fractional free volume for gas separation membranes. *J Mater Chem A.* 2014;2(33):13309–20.